

An Adaptive Reduced–Order Chemical Model

J. C. Lee*, H. N. Najm, S. Lefantzi, J. Ray,

Sandia National Laboratories, 7011 East Ave, MS9051, Livermore, CA 94550, USA.

M. Frenklach

University of California at Berkeley & Lawrence Berkeley National Laboratory, Berkeley CA 94720, USA.

M. Valorani

University of Rome “La Sapienza”, 00184 Roma, Italy.

and D. A. Goussis

Agiou Georgiou 49, 26500 Rio, Greece.

1 Introduction

We demonstrate a new strategy for construction of an adaptive chemistry model. The technique is based on a slow manifold projection scheme derived from computational singular perturbation (CSP) combined with the Piecewise Reusable Implementation of Solution Mapping (PRISM) [1–3]. PRISM is used to tabulate the response surfaces of the CSP tensors. We examine the effectiveness of this scheme by considering a model problem with variable stiffness. We find that, while the degradation in accuracy is minimal, the CPU-cost of the CSP projection method can potentially be reduced substantially using this tabulation strategy, which bypasses the CPU-intensive CSP analysis. Furthermore, we find that the size of the hypercubes used to build the PRISM tabulation can be very large and their dimensionality can be reduced. The dimensionality reduction is achieved by collapsing the dimensions corresponding to the CSP-radicals. This reduction in the hypercubes’ dimensionality is a key aspect of the new strategy.

We deal with a general dynamical system defined as a set of ODEs

$$\frac{d\vec{Y}}{dt} = \vec{g}(\vec{Y}), \quad \vec{Y} \in \mathfrak{R}^N, \quad \vec{g}: \mathfrak{R}^N \rightarrow \mathfrak{R}^N \quad (1)$$

with a large spectral radius, i.e. stiff. CSP analysis starts with a timescale decomposition as follows: an ascending sequence of time scales $\tau_1 \leq \tau_2 \leq \dots \leq \tau_N$ and the corresponding sequence of vectors and co–vectors $\{ \langle \vec{\mathbf{a}}_i, \vec{\mathbf{b}}_i^* \rangle \mid i = 1, \dots, N \}$ [4–10], are used to construct a tensor Q_s to make Eqn. (1) non-stiff: $d\vec{Y}/dt = Q_s \vec{g}(\vec{Y})$, $Q_s = I - \sum_{r=1, M} \vec{\mathbf{a}}_r \vec{\mathbf{b}}_r^*$, where M is the number of exhausted modes or the number of modes that are in “quasi–equilibrium” [6]. This forms the basis of the CSP–projection scheme, first proposed by Valorani and Goussis [5], which consists of 3 steps.

1. Obtain the CSP–slow–manifold projection tensor Q_s and the radical correction tensor R_c (see step 3) using the solution at the current time; $\vec{Y}(t)$ and estimate the proper time step size using τ_{M+1} .
2. Use an explicit step to advance $\vec{Y}(t)$ to $\vec{Y}^*(t + \delta t)$ using the modified source term $Q_s \vec{g}(\vec{Y}(t))$.
3. Evaluate the contribution of the exhausted modes (to leading order) using the “radical correction” [11] i.e. $\vec{Y}(t + \delta t) = \vec{Y}^*(t + \delta t) - R_c \vec{g}(\vec{Y}^*(t + \delta t))$, where the radical correction tensor is defined as $R_c = \sum_{r=1}^{r=M} \vec{\mathbf{a}}_r \tau_r \vec{\mathbf{b}}_r^*$.

Out of the three steps, #1 is most computationally intensive if the CSP analysis is carried out in full. The CSP analysis used here, an improved direct method, is based on a combination of a Singular Value Decomposition (SVD), an eigen–solve, and a direct matrix inversion. The SVD step is taken to improve the condition number associated with the inversion step to obtain the co–vectors. To carry out the projection scheme, we only need two tensors Q_s and R_c .

*Corresponding author: jclee@ca.sandia.gov (Fax:) 925 294 2595 (Tel:) 925 294 4797

The key point in the present development is the construction of efficient models for these two tensors to bypass a direct CSP solve. Step #2 is an efficient explicit scheme stabilized by the CSP tensors when time step size commensurate with τ_{M+1} – not τ_1 – is used. In a series of numerical experiments on dynamically strained premixed flames, we found that the CSP–slow–manifold does not change significantly in space (in the flame–normal coordinate). In fact, the flame–normal coordinate can be partitioned into 25 parts such that, within each, the CSP–slow–manifold varies within $\pm 5\%$. In addition, the CSP–slow–manifold varies with the “slow” time scale (τ_{M+1}); thus, when we use the PRISM technique to tabulate Q_s and R_c , we can use large design factors (“big” hypercubes); furthermore, we can reduce the dimensionality of the hypercubes by collapsing the dimensions associated with the CSP–radicals [6]. The large design factor and the dimensionality reduction in the hypercubes are made possible by the CSP procedure and they offer distinct advantages over the traditional use of PRISM in tabulating the integrated results.

2 Model Problem

We will demonstrate this new CSP-PRISM technique with a 4-D model problem:

$$\frac{dY_i}{\delta t} = \frac{1}{\epsilon^{N-i}} \left(-Y_i + \frac{Y_{i+1}}{1 + Y_{i+1}} \right) - \sum_{j=i+1}^{j=N} \left(\frac{Y_{j+1}}{(1 + Y_{j+1})^2} \right), \quad i = 1, \dots, N; \quad \epsilon \ll 1 \quad (2)$$

where $N = 4$ and $\tau^i = \epsilon^{N-i}$. The CSP–slow–manifolds are defined (to leading order) by $Y_i - Y_{i+1}/(1 + Y_{i+1}) = 0$ when the i^{th} mode becomes exhausted; and the associated CSP–radical is Y_i . Consider the case when $M = 1$. We tabulate Q_s and R_c by taking samples in the hypercube which is expanded only in the dimensions of $\{Y_2, Y_3, Y_4\}$; while Y_1 is evaluated with $Y_1 = Y_2/(1 + Y_2)$. Obviously, if $M = 2$, we can use a two-dimensional hypercube (expanding only Y_3 and Y_4) and a similar expression to evaluate Y_2 . Table 1 presents a 3-parameter 18-run d -optimal design [12]. We construct a *single* hypercube tabulation,

run #	X_2	X_3	X_4	run #	X_2	X_3	X_4
1	0	-1	-1	10	1	-1	-1
2	1	-1	1	11	1	0	-1
3	1	-1	0	12	-1	-1	0
4	-1	-1	1	13	1	1	0
5	1	1	1	14	0	1	1
6	-1	-1	-1	15	1	0	1
7	-1	1	-1	16	0	-1	1
8	-1	0	1	17	-1	1	1
9	1	1	-1	18	0	0	0

Table 1: A three-variable fractional factorial design with 18 runs

where $X_i = \log(Y_i/Y_i^c)/\log f$, $i = 2, 3, 4$ (a log–scaled design); Y_i^c is the center point of the hypercube; the design factor is $f = 10$, which corresponds to a *very large* hypercube; and the dimension of X_1 is *not* expanded.

We first consider the accuracy of the underlying projection method itself. The log–log graph on the left in Fig. 1 indicates that the CSP–slow–manifold projection method is highly accurate ($\mathcal{O}(10^{-5})$ errors are readily obtainable) even when the system is moderately stiff, the CSP tolerance parameters chosen are moderately stringent, and an aggressive time step size is used. The relative error is given by $\bar{E}_{L_2} = \frac{1}{N \cdot N_s} \left[\sum_{n=1, i=1}^{n=N_s, i=N} \left((Y_i(t_n) - Y_i^{ref}(t_n))/Y_i^{ref}(t_n) \right)^2 \right]^{1/2}$ where N_s is the number of time steps taken, and Y_i^{ref} is the reference solution which was calculated (to machine accuracy) with the backward–difference implicit method. The accuracy of the underlying projection scheme is dependent on the tolerance parameters used to perform the CSP analysis itself, and an additional parameter μ that determines

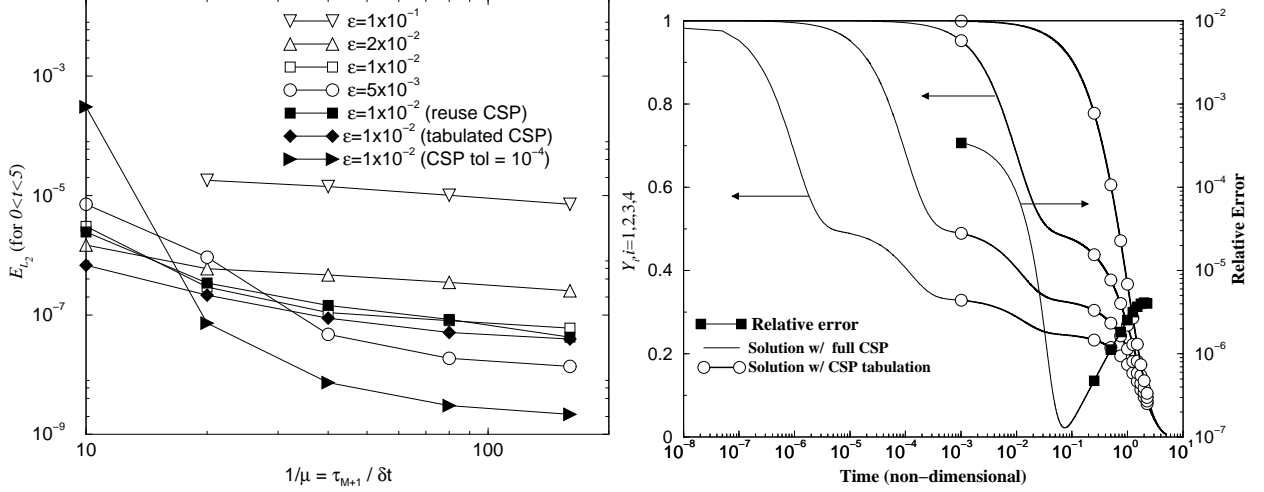


Figure 1: Left: The average L_2 error (\bar{E}_{L_2}) from $t = 0$ to $t = 5$ for the 4-D problem with various values of ϵ integrated with the CSP–projection scheme versus time step sizes. The first four line-plot cases ($\epsilon = 10^{-1}, 2 \cdot 10^{-2}, 10^{-2}, 5 \cdot 10^{-3}$) illustrate the effect of increased stiffness on the L_2 error behavior. The overlaid plots with circle symbols ($\epsilon = 1 \cdot 10^{-2}$), illustrate the effect of reusing the CSP vectors, using the tabulated fast space (not with PRISM, but with a simple linear interpolation technique), and reducing the CSP tolerances, as indicated. Right: Comparison of the solutions of the model problem defined in Eqn. 2 obtained with the original projection scheme with the CSP analysis carried out at every time step in the duration $0 < t < 5$ and the one obtained with the CSP–PRISM strategy i.e. with tensors Q_s and R_c tabulated using the d -optimal design points found in the reduced dimension hypercube (without any CSP analysis) during time integration in the duration $0.001 \leq t \leq 2.34$. The parameters defining the model problem and the time integration procedure are: $\epsilon = 10^{-2}$ and $\mu = 0.05$.

the time step size ($\delta t = \mu \cdot \tau_{M+1}$). In all the plots shown in the LHS graph, Q_s and R_c were evaluated either from first principles at every step or reused until M changes (a CPU cost saving method). We also performed one calculation with the CSP analysis carried out in full in every step and saved the CSP tensors at eight selected points in time (evenly spaced in the time interval $[0, 5]$). We then repeated the same calculation but used these eight sets of data to estimate the CSP tensors by linear interpolation and we report the results in the same figure (curve marked with solid diamonds). It can be observed that the use of approximated CSP tensors by means of the “reuse” strategy or the linear interpolation method did not change the accuracy of the projection scheme significantly. Such a robustness of the projection scheme justifies the proposed tabulation technique.

We now consider the tabulation of the CSP tensors using the CSP–PRISM technique deployed in a reduced–dimension hypercube. We construct second-order polynomial curve fits, with the sampling points shown in Table 1, for components of Q_s and R_c using the standard least-squares method; and store the polynomial coefficients. Here, the time scales τ_i need not be tabulated since they remain constant. In the time integration of the model problem, when the variables fall within the range of validity of a hypercube tabulation, both Q_s and R_c are reconstructed using these polynomials which can be evaluated at a CPU cost substantially lower than the direct CSP analysis. The tabulation can also be pre–constructed to provide additional savings in CPU time.

The single hypercube tabulation so created is valid in the time range of $0.001 \leq t \leq 2.34$ for one of the computations reported in the LHS plot in Fig. 1 – the one with $\epsilon = 10^{-2}$ and $\mu = 0.05$. We also plot, in the RHS graph in Fig. 1, the solution from $t = 0$ to $t = 5$ obtained with the original projection scheme. The solution in $0.001 \leq t \leq 2.34$ calculated with the tabulated CSP tensors is shown delineated with circle symbols. The relative difference between the results obtained with the original projection method and those with the tabulation technique are also reported on the same graph (line with rectangles). It can be seen that the solution obtained is most accurate near the center point used to construct the hypercube tabulation, and that the solution at the end point $t = 2.34$ agrees with those obtained with the full CSP–projection scheme to within 10^{-5} , which is a very promising for a calculation performed with a single large hypercube.

3 Conclusions

We have demonstrated that the combination of the CSP–slow–manifold projection method and PRISM offers a new way to construct an adaptive reduced–order model for a stiff dynamical system. CSP allows not only a reduction in dimensionality, but also using larger hypercubes. By constructing tabulations for the two CSP tensors, we have an efficient explicit time integration construction. The test performed on a stiff model problem demonstrated the feasibility of this novel model construction method. It showed that high level of accuracy is readily achievable. Future work will concentrate on the construction of such an adaptive model for chemical kinetic system that are of relevance to the area of combustion.

Acknowledgments

This work was supported by the US Department of Energy (DOE), Office of Basic Energy Sciences (BES), SCIDAC Computational Chemistry Program. Support was also provided by the DOE BES Division of Chemical Sciences, Geosciences, and Biosciences. Further support was provided by the DOE Office of Advanced Scientific Computing Research, Division of Mathematical, Information and Computational Sciences. Sandia National Laboratories is a multiprogram laboratory operated by Sandia Corporation, a Lockheed Martin Company, for the United States Department of Energy under contract DE-AC04-94-AL85000. M. Frenklach acknowledges the financial support of DOE, BES under contract no. DE-AC03-76SF00098. M. Valorani acknowledges the support of the Italian Space Agency (ASI) and the Italian Ministry of Education, University and Research (MIUR).

References

- [1] S. R. Tonse, N. W. Moriarty, N. J. Brown, and M. Frenklach. PRISM: Piecewise Reusable Implementation of Solution Mapping. An economical strategy for chemical kinetics. *Israel Journal of Chemistry*, 39:97–106, 1999.
- [2] J. B. Bell, N. J. Brown, M. S. Day, M. Frenklach, J. F. Grcar, R. M. Propp, and S. R. Tonse. Scaling and Efficiency of PRISM in Adaptive Simulations of Turbulent Premixed Flames. *Proc. Combust. Inst.*, 28:107–113, 2000.
- [3] S. R. Tonse, M. Moriarty, M. Frenklach, and N. J. Brown. Computational Economy Improvements in PRISM. *Int. J. Chem. Kinet.*, 235:438–452, 2003.
- [4] Ju Y.G. Lu T.F. and Law C.K. *Combustion and Flame*, 126:1445–1455, 2001.
- [5] M. Valorani, H. N. Najm, and D.A. Goussis. CSP analysis of a transient flame-vortex interaction; time scales and manifolds. *Combustion and Flame*, 134:35–53, 2003.
- [6] S.H. Lam and D.A. Goussis. Understanding complex chemical kinetics with computational singular perturbation. In *Proc. Comb. Inst.*, volume 22, page 931, 1988.
- [7] H. G. Kaper and T. J. Kaper. Asymptotic analysis of two reduction methods for systems of chemical reactions. *Physica*, 165:66–93, 2002.
- [8] D.A. Goussis and S.H. Lam. On the homogeneous methane-air reaction system. Report 1892-MAE, Princeton Univ., 1990.
- [9] S.H. Lam and D.A. Goussis. Conventional asymptotics and computational singular perturbation for simplified kinetics modelling. In M.O. Smooke, editor, *Reduced Kinetic Mechanisms and Asymptotic Approximations for Methane-Air Flames*, number 384 in Springer Lecture Notes. Springer Verlag, 1991.
- [10] J. J. Levin and N. Levinson. Singular perturbations of nonlinear system terms of differential equations and an associated boundary layer equation., *J. Rat. Mech. Anal.*, 3:247–270, 1954.
- [11] M. Valorani, D.A. Goussis, and H.N. Najm. Using csp to analyze computed reactive flows. In *8th SIAM Int. Conf. On Numerical Combustion*, Amelia Island, FL, March 2000.
- [12] A.C. Atkinson and A.N. Donev. *Optimum Experimental Design*. Oxford Univ. Press, UK, 1992.